The Aortomitral Angle is Suspended by the Anterior Mitral Basal "Stay" Chords

W. A. Goetz[1]
H.-S. Lim[2]
E. Lansac[3]
P. A. Weber[2]
D. E. Birnbaum[1]
C. M. G. Duran[2]

Abstract

Objectives: The function of the anterior mitral basal "stay" chords (SC) is not yet known. Collagen fiber orientation of the anterior mitral leaflet (AML) suggests that local stress is directed from papillary muscles (PM) over SC and AML to fibrous trigones (FT), maintaining the aortomitral angle (AMA). It has been shown that narrowing of AMA increases risk of systolic anterior movement (SAM). **Methods:** Sonomicrometry crystals were implanted in six sheep at the left ventricular (LV) apex, PM tips (M1, M2), FT (T1, T2), posterior mitral annulus (PMA), and base of aortic right coronary sinus (RCS). The retracting force of ascending aorta was measured. **Results:** Transection of SC resulted in an increase of distance M1-T1 and M2-T2. Consequently, the AMA narrowed at end systole by $-3.26 \pm 0.85^\circ$ ($p < 0.05$) and at end diastole by $-4.16 \pm 1.28^\circ$ ($p < 0.05$). A force of 1.8 ± 0.2 N was needed to pull the recoiling ascending aorta back to its original position. **Conclusions:** The elastic recoil of ascending aorta is balanced by SC, which connect PM to FT and constitute the center of the LV base. Transection of SC narrows AMA and increases the risk of SAM.

Key words
Aortomitral angle · mitral valve · anterior basal chordae tendinae · stay chords · sonomicrometry

Introduction

The function of the marginal mitral valve chords is to maintain mitral leaflet apposition during valve closure [1]. The function of the anterior basal chords is unclear, but has been shown to support the belly of the anterior leaflet [2]. These basal, or second-order, chords defined by Tandler [3] arise from each papillary muscle (PM) and enter the ventricular aspect of the anterior mitral leaflet (AML). Among these basal chords, two particularly thick, tendon-like chords stretch from the PM to the undersurface of the anterior leaflet close to the anterior mitral annulus [4]. In a model with isolated, perfused pig hearts, van Rijk-Zwikker et al. [5] demonstrated that these two chords, termed "stay chords" (SCs) [4], remain tense during the entire cardiac cycle.

In an anatomic study of 50 adult human hearts, Lam et al. [6] found these two "principal" or "strut" chords to be the longest and thickest of all chords. Several authors have shown that transection of all anterior basal chords or the two principal second-order chords does not result in mitral valve regurgitation or change in leaflet coaptation [1, 7].

Affiliation
[1] Klinik für Herz-, Thorax- und herznahe Gefäßchirurgie, Klinikum der Universität Regensburg, Germany
[2] The International Heart Institute of Montana Foundation at St. Patrick Hospital and Health Sciences Center and The University of Montana, Missoula, Montana, USA
[3] Chirurgie Thoracique et Cardiovasculaire, Hopital Pitie-Salpetriere, Paris, France

Dedication
This paper was presented at the 32nd Annual Meeting of the German Society for Thoracic and Cardiovascular Surgery, 23 – 26 February 2003 in Leipzig, Germany; Abstract ID: 16057

Correspondence
Carlos M. G. Duran, MD, PhD· The International Heart Institute of Montana · 554 West Broadway · Missoula, Montana 59802 · USA · Phone: + 1/406/329-5668 · Fax: + 1/406/329-5880 · E-mail: duran@saintpatrick.org

Received March 27, 2003

Bibliography
Thorac Cardiov Surg 2003; 51: 190–195 · © Georg Thieme Verlag Stuttgart · New York · ISSN 0171-6425

Although the SCs' function is not yet known, they are often sectioned, transferred to the leaflet margin, and assumed to be irrelevant to left ventricular (LV) geometry or mitral valve function in surgical procedures [8].

Cochran and associates [9] investigated the distribution and direction of the collagen fibers within the AML. They found that the collagen fibers in the central portion of the AML run parallel to the annulus. In the lateral aspects of the leaflet, the fibers are oriented from the insertion of the SCs toward the fibrous trigones (FTs). This finding suggests that the SCs connect the PM to both FTs under tension.

The FTs are located at the connection of the aortic and mitral annulus and form the hinge axis of the aortomitral plane. They are connected cranially to the ascending aorta, and the SCs link the FTs with the PM over the AML. In this way, a line from the PM to the ascending aorta is formed, which possibly maintains the architecture of the LV base and the aortomitral angle (AMA). When the ascending aorta is sectioned, it recoils. The recoiling force of the ascending aorta is probably counterbalanced by the SCs. Transection of the SCs should result in a pull on the trigones and narrowing of the AMA.

The present study is an attempt to confirm the hypothesis that the SCs play an essential role in maintaining the normal AMA; consequently, their section would increase the risk of systolic anterior mitral leaflet motion (SAM) after mitral valve repair.

This subject is particularly interesting at a time when the function of the SCs is controversial. Although some authors find them of little consequence [7,10], others suggest their surgical transection to abolish the leaflet tethering present in functional mitral regurgitation [11].

Materials and Methods

Six Targhee sheep (58 ± 18 kg) (mean ± SD) underwent implantation of 7 ultrasonic crystals (Fig. **1**) using cardiopulmonary bypass. All animals received humane care in accordance with the Principles of Laboratory Animal Care formulated by the Animal Welfare Act in the Guide for Care and Use of Laboratory Animals prepared by the Institute of Laboratory Animal Resources and published by the National Institutes of Health (NIH publication #85–23, revised 1996). This project was also reviewed and approved by the Institutional Animal Care and Use Committee (IACUC) of The University of Montana.

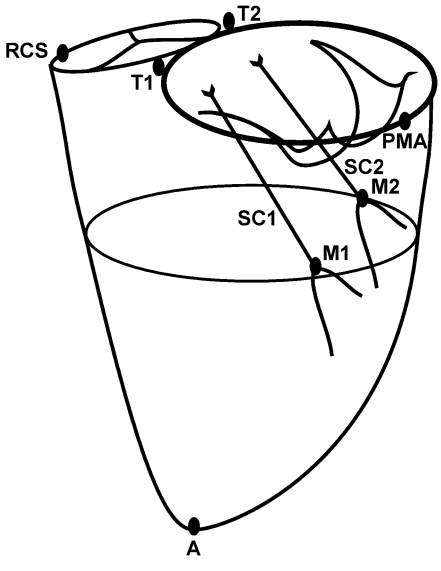

Fig. **1** Diagram showing crystal locations at: A: apex, M1: anterolateral papillary muscle tip, M2: posteromedial papillary muscle tip, RCS: right coronary sinus, T1: anterior trigone, T2: posterior trigone, PMA: midpoint of posterior mitral annulus, SC1: anterolateral stay chord, SC2: posteromedial stay chord.

Surgical Protocol

The sheep were premedicated with Ketamine (1.0 mg/kg) and Propofol (4.0 mg/kg). Artificial ventilation was achieved using a volume-regulated respirator (North American Drager, Telford, PA, USA). ECG was monitored continuously with 5 leads. Anesthesia was maintained with intermittent Propofol i.v. and Isoflurane at a gas level of 0.5% to 2.5% as needed. The heart was exposed with a standard left thoracotomy through the fourth intercostal space and a T-shaped incision of the pericardium. An arterial line was placed in the aortic arch for blood pressure monitoring. In preparation for cardiopulmonary bypass, a bolus injection of Heparin at 300 U/kg was administered i.v. with a target ACT of 480 seconds or more. The ascending aorta was cannulated with a #16 Fr arterial cannula, and a #32 Fr dual stage single venous cannula (Medtronic, Inc., Minneapolis, MN, USA) was inserted into the right atrium. After starting cardiopulmonary bypass, an LV vent was inserted through the LV apex. The ascending aorta was cross-clamped, followed by infusion of cold blood cardioplegia into the aortic root.

Seven 2-mm ultrasonic crystals (Sonometrics Corporation, London, Ontario, Canada) were implanted and secured with 5/0 polypropylene sutures at: 1) LV apex; 2) both PM tips (M1 and M2); 3) midpoint of the posterior mitral annulus (PMA); 4) both FT (T1 and T2); and 5) the base of right coronary sinus (RCS) (Fig. **1**).

All electrodes of the crystals on the mitral annulus were exteriorized through the left atriotomy. PM electrodes were exteriorized through the apex. The electrode of the RCS was exteriorized through the aortotomy. Two insulated wires were placed around the SCs close to their leaflet insertion. The part of the wires in contact with the chords was denuded. Both wires were exteriorized through the LV septum and right ventricular outflow tract to prevent injury to other basal or marginal chords when diathermy was applied to them. A high fidelity, catheter-tipped pressure transducer (Model 510, Millar Instruments, Houston, TX, USA) was placed within the lumen of the proximal ascending aorta and in the LV cavity through the apex.

After weaning from cardiopulmonary bypass, the venous and arterial cannulas were removed, and heparin was neutralized with protamine. Baseline recordings were taken under hemodynamically stable conditions (at least 30 minutes after weaning from cardiopulmonary bypass). Sectioning of the two SCs was achieved in the beating heart by applying diathermia to the two wires placed around the SCs close to their leaflet insertion. A second set of data was then recorded. Epicardial echocardiography was performed before and after chordal transection to detect the possible presence of mitral incompetence. At the end of the

experiment, the heart was explanted, and the recoiling force of the ascending aorta was measured with a Newton spring scale.

Definition of the Phases of the Cardiac Cycle

Geometric changes were time related to each phase of the cardiac cycle defined from the aortic and LV pressure curves. End diastole or beginning of systole was defined as the point of increasing LV pressure tracing (dP/dt > 0). End of isovolumic contraction was defined as the beginning of ejection at the crossing point of the LV and aortic pressure curves (gradient aortic/LV pressure = 0). The dicrotic notch in the aortic pressure curve defined end systole. End diastole was defined as the lowest point of LV pressure tracing after ejection (dP/dt = 0) [12].

Definition of Anatomic Regions and Calculations

Distances between crystals were explored in a coordinate-independent analysis [13]. Insertion of the SCs on the PM was defined as the origin of the SCs (M1 and M2). The anterior (T1) and posterior (T2) FTs were identified by pulling on the midpoint of the AML, which created folds terminating at the trigones. The mitral annulus plane was defined as plane that included both FTs (T1 and T2) and the middle of the posterior mitral annulus (PMA). The aortic annulus plane was defined as plane incorporating both FTs (T1 and T2) and the lowest point of the RCS (Fig. **2**). Both planes defined the base of the heart with the hinge at the axis between the FTs (T1 and T2). The AMA was defined as the angle formed by the aortic and mitral annulus planes and was calculated by a line traced between RCS and the midpoint between T1 and T2 and another traced between PMA and the midpoint between T1 and T2, with the apex of the angle at the axis between T1 and T2 (Fig. **2** and **3**).

Data Acquisition

Distances were measured with Sonometrics Digital Ultrasonic Measurement System TRX Series using transmitter/receiver crystals. A post-processing program (Sonometrics Corporation, London, Ontario, Canada) was used to examine each individual length tracing between crystals and for three-dimensional (3D) reconstruction of the crystal coordinates. The data sampling rate was 200 Hz. Millar pressure transducer control units TCB 600 and MIKRO-TIP pressure transducers (Millar Instruments, Inc. Houston, TX, USA) were used to obtain the LV and aortic pressures. All other pressure measurements were taken directly by inserting a 20-gauge needle and using a conventional pressure transducer. A Swan-Ganz catheter (Baxter Healthcare Corporation, Edwards Critical-Care, Irvine, CA, USA) was used to acquire pulmonary artery pressure and cardiac output. All distances, pressures, and flows were displayed and recorded simultaneously on the same screen by the Sonometrics system. This ensured that all data were synchronized and recorded on the same timeline. Epicardial two-dimensional (2D) echocardiography with PW- and color-Doppler was used to determine the presence of mitral regurgitation before and after chord transection.

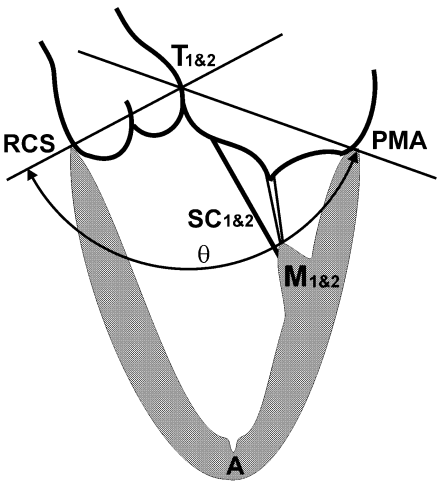

Fig. **2** Left ventricle and aortomitral angle (Θ) at baseline (end diastole: 150.73 ± 15.48°, end systole: 139.66 ± 16.87°) SC: stay chord, A: apex, M1: anterolateral papillary muscle tip, M2: posteromedial papillary muscle tip, RCS: right coronary sinus, T1: anterior trigone, T2: posterior trigone, PMA: midpoint of posterior mitral annulus.

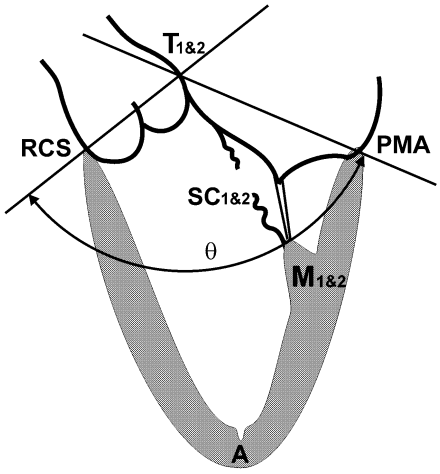

Fig. **3** Left ventricle and aortomitral angle (Θ) after transection of stay chords (SC) (end diastole: 146.57 ± 14.95°, end systole: 136.40 ± 17.22°). The aortomitral angle narrowed after transection of stay chords in diastole by – 4.2 ± 1.3° and in systole by – 3.3 ± 0.8°. A: apex, M1: anterolateral papillary muscle tip, M2: posteromedial papillary muscle tip, RCS: right coronary sinus, T1: anterior trigone, T2: posterior trigone, PMA: midpoint of posterior mitral annulus.

Measurement and Statistical Analysis Methods

After close examination of the data, three consecutive heartbeats that contained the least amount of noise were chosen for analysis. The summary statistics are reported as mean ± standard deviation. Hemodynamic and geometric measures were compared using the two-tailed t-test for paired comparisons (baseline versus chordal transection), with a significance level of $p < 0.05$ (corrected by Stepdown Bonferroni for multiple pair wise comparisons). Statistical analyses were done by using SAS 8.2 PROC MULTTEST software (SAS Institute, Inc., Cary, NC, USA).

Results

Before and immediately after transection of the SCs, no mitral regurgitation was detected by echocardiography. None of the other measured hemodynamic parameters revealed any significant difference after transection of the SCs (Table **1**). Postmortem,

Tab. **1** Hemodynamic measurements and mitral regurgitation by echocardiography before and after transection of stay chords

hemodynamic measurements	*baseline*	*after transection*
heart rate beats/min	108.7±14.3	110.1±14.3
central venous pressure (mmHg)	10.2±1.6	10.8±1.2
left atrial pressure (mmHg)	9.3±1.2	9.8±1.3
LV systolic pressure (mmHg)	95.5±10.9	97.9±14.1
LV end diastolic pressure (mmHg)	14.8±5.2	16.5±1.6
systolic aorta pressure (mmHg)	87.3±10.7	89.9±17.2
diastolic aorta pressure (mmHg)	48.1±4.9	46.8±7.5
mean aorta pressure (mmHg)	61.2±5.3	63.0±7.9
systolic pulmonary artery pressure (mmHg)	24.8±5.4	25.2±5.9
diastolic pulmonary artery pressure (mmHg)	12.7±3.4	13.3±3.4
mean pulmonary artery pressure (mmHg)	16.7±3.3	17.3±3.1
cardiac output (l/min)	4.7±0.7	4.6±1.2
cardiac index (l/min/m^2)	4.0±1.5	3.9±1.4
Systemic Vascular Resistance (dyns/cm^5/m^2)	1245.1±847.2	1252.2±833.2
mitral regurgitation by echo-cardiography	0	0

the hearts were explanted and the recoiling force of the ascending aorta was measured. An average force of 1.8±0.2 N was needed to pull the aortic root back to its original position. An incremental force of 1.8±0.1 N was necessary to pull it 10 mm further toward the apex of the heart. Examination of the heart showed crystals in the correct position and the SCs transected about 2 to 3 mm from their leaflet insertion. The other basal and marginal chords were intact.

Sonomicrometry Results

At baseline, all distances between apex and LV base shortened significantly during systole. Only distances between origins of the SCs (M1 and M2) on PM tips to FT (T1 and T2) increased (Table **2**). These findings represent normal systolic tension on the SC [14].

Immediately after transection of the SCs (Fig. **3**), the distance M1–T1 increased by +0.85±0.35 mm at end diastole ($p < 0.05$) and by +0.96±0.41 mm at end systole ($p < 0.05$). The distance M2–T2 increased by +0.77±0.26 mm at end diastole ($p < 0.05$) and by +0.97±0.42 at end systole ($p < 0.05$) (Table **3**).

SC transection was followed by an increase in LV length. Distance LV apex to trigones (T-A) increased at T1-A by +1.04±0.53 mm ($p < 0.05$) at end diastole and by +1.14±0.60 mm ($p < 0.05$) at end systole. T2-A increased by +1.02±0.38 mm ($p < 0.05$) at end-diastole and by +0.97±0.37 mm ($p < 0.05$) at end systole. However, this overall increase in LV length was not uniform. Distances between LV apex (A) and PMA and RCS did not change significantly after transection of the SCs. Therefore, increase in LV length was exclusively due to the increase in distance between PM tips and FT. This resulted in a change of the AMA. After transection of the SCs, the AMA narrowed by –4.16±1.28° ($p < 0.05$) during end diastole and by –3.26±0.85° ($p < 0.05$) during end systole (Table **3**).

Discussion

Although recognized for a long time in anatomic studies [3], the function of the anterior mitral basal (or second-order) chords is unknown. They are often excised in valve replacement or transferred to the free margin [8]. Markus et al. [2] suggested that their function was to support the leaflet belly to avoid its ballooning.

Among the basal chords, there are two particularly thick chords described in the anatomic literature as “principal” or “strut” chords [15]. In a study of 50 adult human hearts, Lam et al. [6] showed that these two chords were the longest and thickest of all chords.

Recent videofluoroscopy studies in normal sheep have shown that the distance between PM and mitral annulus remained constant throughout the cardiac cycle [16]. The observation of a video produced by van Rijk-Zwikker et al. [5] suggested that the strut chords must be responsible for this constant annulopapillary distance. This videoscopic study performed in isolated working pig hearts showed the presence of two thick anterior basal chords that remained under tension during the entire cardiac cycle, although this tension is not linear throughout the cardiac cy-

Tab. **2** Distances at baseline and after transection of stay chords at end diastole and end systole

distances	*baseline*		*after transection*	
	end diastole	*end of systole*	*end diastole*	*end of systole*
M1-T1 (mm)	28.88±5.32	30.47±5.61	29.73±5.31	31.42±5.93
M2-T2 (mm)	33.37±2.08	34.38±1.88	34.14±1.92	35.35±1.93
T1-A (mm)	93.91±11.75	88.77±12.00	94.95±11.64	89.91±11.23
T2-A (mm)	89.86±11.96	85.83±11.40	90.88±12.00	86.80±12.15
PMA-A (mm)	84.79±12.75	77.82±11.79	85.64±12.83	78.49±11.16
RCS-A (mm)	94.89±13.43	89.28±12.71	95.03±13.30	89.01±12.18
aortomitral angle (deg)	150.73±15.48	139.66±16.87	146.57±14.95	136.40±17.22

M: papillary muscle tip; T: trigones; A: LV apex; PMA: posterior mitral annulus; RCS: right coronary sinus

Tab. **3** Change in distances from baseline to after transection at end diastole and end systole

distances	*end diastole*	*end of systole*
M1-T1 (mm)	+ 0.85 ± 0.35*	+ 0.96 ± 0.41*
M2-T2 (mm)	+ 0.77 ± 0.26*	+ 0.97 ± 0.42*
T1-A (mm)	+ 1.04 ± 0.53*	+ 1.14 ± 0.60*
T2-A (mm)	+ 1.02 ± 0.38*	+ 0.97 ± 0.37*
PMA-A (mm)	+ 0.84 ± 0.55	+ 0.68 ± 1.26
RCS-A (mm)	+ 0.14 ± 0.58	– 0.19 ± 0.80
aortomitral angle (deg)	– 4.16 ± 1.28*	– 3.26 ± 0.85*

M: papillary muscle tip; T: trigones; A: LV apex; PMA: posterior mitral annulus; RCS: right coronary sinus. *p-value ≤ 0.05

Tab. **4** Force on recoiling aorta at original position (0 mm) and after pulling it 10 mm toward the apex of the left ventricle

Position aorta	*0 mm*	*10 mm*
Average force	1.8 ± 0.2 N	1.8 ± 0.1 N

cle [17]. In every mitral valve anatomically studied or surgically explored, there were two recognizable tendon-like chords we termed "stay chords" [4]. Recently, in a study of the distribution and direction of the collagen fibers within the AML, Cochran and associates [9] have shown that these fibers are oriented from the region of insertion of the SCs toward the FTs. This finding suggests that the SCs connect the PMs to both FTs under tension.

Our present study provides an anatomic basis for the previously reported constant distance between the PM and mitral annulus [13,16]. Selective transection of the SCs significantly increased this distance. This increase in distance determined an overall LV lengthening (apex-trigones) without a distance change from apex to PMA or apex to RCS.

In both the isolated pig heart preparation and echocardiograms of normal humans, we have observed that the SCs are in a straight line that stretches from the PM tips to the aortic curtain and ascending aorta, including the FTs. We also observed in the sheep heart that when the aorta was completely transected at the sinotubular junction, the aorta recoiled cranially. An average force of 1.8 ± 0.2 N was needed to pull the aortic root back to its original position. An incremental force of 1.8 ± 0.1 N was necessary to pull it 10 mm further toward the apex of the heart.

Tension on the SCs was recently measured by Nielsen et al. [17], who showed a force of 0.56 ± 0.09 N acting on the anterior and 0.88 ± 0.13 N on the posterior SC. We hypothesized that the elastic recoil of the ascending aorta is balanced at the center of the LV base by the SCs, which connect the PM to the ascending aorta through the aortic curtain and FTs. This mechanism maintains the AMA during the entire cardiac cycle, including the systolic descent of the atrioventricular plane [18].

In the present study, transection of the SCs (as regularly used for chordal transfer in mitral valve repair) resulted in a significant narrowing of the AMA because the elastic recoil of the ascending aorta was no longer balanced by the pull of the SCs at the trigones.

Narrowing of the AMA can also be observed after implantation of mitral valve prostheses. Because of AMA narrowing due to mitral valve replacement, the mitral inflow pattern in the LV will be reversed. In a normal pattern, the flow seen in late diastole has the same direction as the systolic ejection flow. When reverse flow occurs, LV inflow is directed toward the septum and, therefore, into the LV outflow tract so the outflow is displaced posterolaterally into the LV inflow region [19].

Mihaileanu et al. [20] also found that the AMA narrows after implantation of a rigid mitral annuloplasty ring. Consequently, they observed the same phenomena of reversed flow pattern in the LV, which moves the AML toward the septum and blocks the LV outflow tract. The authors proposed this mechanism as responsible for the presence of systolic anterior mitral leaflet motion (SAM) after mitral annuloplasty.

Our data suggest that the simultaneous transection and transfer of the SCs will additionally narrow the AMA and further increase the risk for SAM in mitral annuloplasty. These findings are particularly important at a time when transection of the SC is being proposed as a surgical therapy for functional mitral regurgitation [11].

Limitations of the study

Our findings are drawn from a limited number of LV markers that only included three markers on the anterior leaflet. Present technology limits the number of crystals. Moreover, the markers and their electrodes might interfere with the normal movements of the different structures. An effort was made to exteriorize the electrodes away from the mitral valve. Variability among animals in the position of the crystals was a concern that was minimized by having a single surgeon performing all surgeries. Also, the data were obtained in an anesthetized, open chest, acute animal model studied immediately after cardiopulmonary bypass and cardioplegic arrest. These obviously non-physiological conditions limit the value of our findings. All data were obtained under the same conditions before and immediately after chordal transection, which advocates for the reliability of the data. It must be emphasized that our findings in sheep cannot necessarily be applicable to the human heart. Sheep have relatively thinner SCs than humans; therefore, the role of the SCs may be more pronounced in humans. Species differences and experimental conditions forbid the uncritical transfer of these findings to the clinical setting.

Conclusions

The elastic recoil of the ascending aorta is balanced by the two main anterior mitral basal chords or SC. These chords connect the PM to the FT, which constitutes the center of the LV base. Se-

lective transection of the two anterior SCs resulted in an increase in the distance between PM tips and FT and, consequently, in narrowing of the AMA. As shown by other authors, narrowing the AMA increases the risk of post-repair systolic anterior motion (SAM). We hypothesize that in mitral annuloplasty, the simultaneous transection and transfer of SCs further increases the risk of SAM.

Acknowledgments

We appreciate the unconditional help of Leslie Trail, Holly Meskimen, and Lorinda Smith in the animal laboratory, of Travis Togo for collecting and handling the sonometric data, and the editorial assistance of Jill Roberts.

Dr. Goetz was supported by a grant from Max Kade Foundation Inc., New York, USA and Deutsche Forschungsgemeinschaft, Bonn, Germany. Mr. Lim was supported by grant ARC 13/96 from the Singapore Ministry of Education and Nanyang Technological University.

References

[1] Obadia JF, Casali C, Chassignolle JF, Janier M. Mitral subvalvular apparatus: different functions of primary and secondary chordae. Circulation 1997; 96: 3124 – 3128

[2] Marcus RH, Sareli P, Pocock WA, Meyer TE, Magalhaes MP, Grieve T, Antunes MJ, Barlow JB. Functional anatomy of severe mitral regurgitation in active rheumatic carditis. Am J Cardiol 1989; 63: 577 – 584

[3] Tandler J. Handbuch der Anatomie des Menschen. Jena: Gustav Fischer, 1913

[4] Kumar N, Kumar M, Duran CM. A revised terminology for recording surgical findings of the mitral valve. J Heart Valve Dis 1995; 4: 70 – 75; Discussion 76 – 77

[5] van Rijk-Zwikker GL, Delemarre BJ, Huysmans HA. Mitral valve anatomy and morphology: relevance to mitral valve replacement and valve reconstruction. J Card Surg 1994; 9: 255 – 261

[6] Lam JH, Ranganathan N, Wigle ED, Silver MD. Morphology of the human mitral valve. I. Chordae tendinae: a new classification. Circulation 1970; 41: 449 – 458

[7] Timek TA, Nielsen SL, Green GR, Dagum P, Bolger AF, Daughters GT, Hasenkam JM, Ingels NB Jr, Miller DC. Influence of anterior mitral leaflet second-order chordae on leaflet dynamics and valve competence. Discussion 541. Ann Thorac Surg 2001; 72: 535 – 540

[8] Carpentier A. Cardiac valve surgery – the "French correction". J Thorac Cardiovasc Surg 1983; 86: 323 – 337

[9] Cochran RP, Kunzelman KS, Chuong CJ, Sacks MS, Eberhart RC. Nondestructive analysis of mitral valve collagen fiber orientation. ASAIO Trans 1991; 37: M447 – M448

[10] Obadia JF, Janier M. Second order anterior mitral leaflets play a role in preventing systolic anterior motion. Ann Thorac Surg 2002; 73: 1689 – 1690; Discussion 1690

[11] Messas E, Guerrero JL, Handschumacher MD, Conrad C, Chow CM, Sullivan S, Yoganathan AP, Levine RA. Chordal cutting: a new therapeutic approach for ischemic mitral regurgitation. Circulation 2001; 104: 1958 – 1963

[12] Guyton AC. Textbook of Medical Physiology, 9th ed. Philadelphia, PA: WB Saunders, 1996

[13] Dagum P, Timek TA, Green GR, Lai D, Daughters GT, Liang DH, Hayase M, Ingels NB Jr, Miller DC. Coordinate-free analysis of mitral valve dynamics in normal and ischemic hearts. Circulation 2000; 102: III62 – III69

[14] Kunzelman KS, Cochran RP. Mechanical properties of basal and marginal mitral valve chordae tendinae. ASAIO Trans 1990; 36: M405 – M408

[15] Yacoub M. Anatomy of the mitral valve chordae and cusps. In: Kalmanson D (ed). The Mitral Valve. Acton, MA: Publishing Sciences Group, 1976: 15 – 20

[16] Komeda M, Glasson JR, Bolger AF, Daughters GT 2nd, Ingels NB Jr, Miller DC. Papillary muscle-left ventricular wall "complex". J Thorac Cardiovasc Surg 1997; 113: 292 – 300; Discussion 300 – 301

[17] Nielsen SL, Green GR, Dagum P, Timek T, Bolger AF, Hasenkam JM, Ingels NB, Miller DC. Why is the Relationship between Anterior Mitral Leaflet Strut Chordae Tension and Left Ventricular Pressure During Isovolumic Contraction Not Linear? Circulation 1999; 100: I – 575

[18] Alam M, Rosenhamer G. Atrioventricular plane displacement and left ventricular function. J Am Soc Echocardiogr 1992; 5: 427 – 433

[19] Omoto R, Matsumura M, Asano H, Kyo S, Takamoto S, Yokote Y, Wong M. Doppler ultrasound examination of prosthetic function and ventricular blood flow after mitral valve replacement. Herz 1986; 11: 346 – 350

[20] Mihaileanu S, Mariono JP, Chauvaud S, Perier P, Forman J, Vissoat J, Julien J, Dreyfus G, Abastado P, Carpentier A. Left ventricular outflow obstruction after mitral valve repair (Carpentier's technique). Proposed mechanisms of disease. Circulation 1988; 78: I78 – I84